

Table 1

	Payload fraction %	Mission duration, hr	Specific impulse, sec
Arcjet	11	1025	1125
MGD	45	1500	2000
Ion engine	55	2000	3000

propulsion system over the arcjet and the ion engine, therefore, are the shorter mission duration at little sacrifice in payload, or conversely, higher payload fraction with slight increase in mission duration

As an example, with power to weight ratio at 0.01 kw/lb the values as shown in Table 1 are obtained

Table 1 clearly indicates the superior mission capability of the MGD propulsion system for lunar ferry missions. Assuming a 220,000 lb initial weight, the gain in payload with the MGD propulsion system can be nearly 75,000 lb over that of the arcjet with an increase in mission duration of 475 hr. On the other hand, the mission duration can be shortened by 500 hr for a slight reduction of payload (22,000 lb) as compared with the ion engine.

The particular example thus proves decidedly the advantages in using MGD propulsion for lunar ferry missions.

References

- 1 Brown, H. and Nicoll, H. E., Jr., "Electrical propulsion capabilities for lunar exploration," AIAA J 1, 314-319 (1963).
- 2 Brandmaier, H. E., Durand, J. L., Gourdine, M. C., and Rubel, A., "An investigation of a one kilowatt hall accelerator," AIAA Preprint 63046 (March 1963).

Supersonic Magnus Effect on a Finned Missile

EDWARD R. BENTON*

National Center for Atmospheric Research,
Boulder, Colo

A supersonic magnus moment is shown to exist on a cruciform missile whose fins are deflected into an aileron setting. The effect is unusual in that it does not depend on interference, but rather on the normal forces on the two panels that are instantaneously perpendicular to the plane of the angle of attack. The moment is negative, large, and increases as the Mach number decreases toward 1. This agrees with scanty data obtained in 1955 in the aeroballistic range.

Introduction

IN 1955 Nicolaides and MacAllister¹ presented what may well have been the earliest unclassified magnus data for a finned missile (Fig. 23 of Ref. 1). These data were obtained for a configuration known as "the basic finner," which is shown in Fig. 1. The model was gun launched in the free flight ballistic range at the Ballistic Research Laboratory. The fins were canted slightly into an aileron deflection in order to induce the spin that is necessary for the existence of magnus effects. The data obtained are plotted in Fig. 2; they consist of the magnus moment coefficient derivative

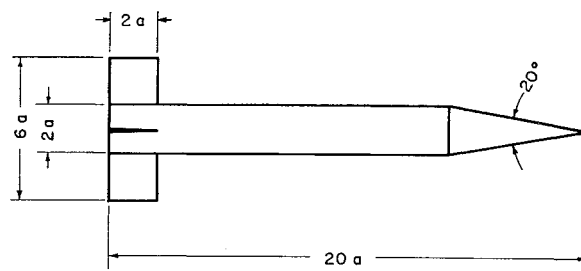


Fig. 1 Basic finner configuration

$C_{M_{p\alpha}}$ as a function of Mach number M . Interesting features of these data are the negative sign, the relatively large magnitude, and especially the large increase in $-C_{M_{p\alpha}}$ as the Mach number decreases toward 1. The author has not seen any explanation for these data. The purpose of this note is to point out the existence of a simple, yet not well known, mechanism that gives rise to magnus moments of the indicated sign, magnitude, and general trend with Mach number.

Known Causes for Magnus Effect

The classical magnus lift on a rotating cylinder and the magnus side force on a spinning missile of revolution at angle of attack both depend on boundary layer effects.^{2,3} These effects are not expected to produce negative moments of the large magnitude observed in Fig. 2 when the main flow becomes supersonic.⁴

In Ref. 5 the author has considered incompressible magnus effects on a missile with both wing and tail fins, showing that wing-tail vortex interference is a source of large, negative magnus forces and moments. However, the basic finner discussed here does not have wing panels to shed vorticity ahead of the tail fins. Moreover, even if the body shed sizable amounts of vorticity which could interact with the tail, there is no reason to expect the sensitive dependence on Mach number exhibited in Fig. 2.

Very recently Platou⁶ has discussed supersonic magnus effects on a finned missile whose maximum fin span equals the maximum body diameter. For such a configuration, wing-body interference is the primary source of magnus effects. Yet wing-body interference on the basic finner should be fairly small because the body radius is only $\frac{1}{3}$ of the wing semispan.^{7,8} Furthermore, during the tests which gave the data of Fig. 2, the pitching and yawing motion was extremely small, and so the cross-flow velocities needed for wingbody interference must not have been large.

Still another source of magnus effects on finned missiles is leading edge suction.⁹ For the rectangular panels of the

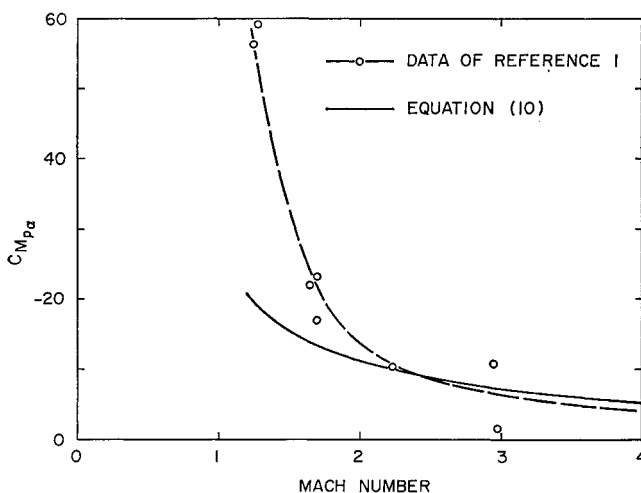


Fig. 2 Magnus moment coefficient derivative as a function of Mach number

Received October 7, 1963

* Staff Scientist, Laboratory of Atmospheric Sciences Member AIAA

basic finner, leading edge suction forces would be nearly parallel to the longitudinal body axis and therefore probably not capable of producing very large moments. Although all of the forementioned sources may be present to some extent in the data of Fig. 2, it seems clear that the dominant contributor is some other mechanism not previously considered.

Noninterference Mechanism for Supersonic Magnus Moment

The mechanism for magnus moments discussed here does not depend on interference, but rather on the normal forces on the two wing panels which are ordinarily incapable of contributing any magnus effects. The existence of such a moment was first pointed out by Bolz¹⁰. We consider the basic finner to be rolling at the steady-state rolling velocity p , which is determined by an exact balance between the roll-damping moment and the rolling moment induced by the deflected fins. Figure 3 shows the nomenclature. The x, y, z coordinate system is fixed at the center of gravity and does not roll with the missile. The figure shows the missile at an instant when two of the fins (1 and 3) are perpendicular to the plane of the angle of attack and the other two fins (2 and 4) are nearly in that plane. Also shown are the forces normal to panels 1 and 3, N_1 and N_3 , respectively. These forces have components parallel to the x axis which contribute a yawing moment about the z axis (i.e., a magnus moment). Since there is no corresponding force in the magnus direction (the y direction), the moment is a pure couple. The usual convention for the sign of magnus moments is that a force in the direction of the classical magnus force on the body alone (the positive y direction for the present case) produces a positive magnus moment if it acts to the rear of the center of gravity. Consequently, positive magnus moments are represented vectorially in the coordinate system of Fig. 3 by arrows in the negative z direction. With this convention the magnus moment which arises because of the forces N_1 and N_3 is simply

$$M_{p\alpha} p\alpha = -N_1 y_1 \sin \delta - N_3 y_3 \sin \delta = -(N_1 y_1 + N_3 y_3) \delta \quad (1)$$

where $M_{p\alpha} p\alpha$ is the magnus moment, p the roll rate, α the body angle of attack, δ the panel deflection, and y_1 and y_3 the spanwise centers of pressure of the forces N_1 and N_3 , respectively.

A chordwise strip of fin 1 between spanwise stations y and $y + dy$ is at an effective incidence $\alpha - \delta + (py/U)$, the last term being the incidence caused by the fins rotating with the missile. Consequently, the total force or moment is found by integrating along the span from $y = a$, the body radius, to $y = 3a$, the spanwise distance to the fin tip:

$$N_1 y_1 = \int_a^{3a} q C_{N\alpha} \left(\alpha - \delta + \frac{py}{U} \right) 2ay dy \quad (2)$$

where q is the dynamic pressure, U the flight velocity, and $C_{N\alpha}$ the slope of the normal force curve. For fin 3, the corresponding expression is

$$N_3 y_3 = \int_a^{3a} q C_{N\alpha} \left(\alpha + \delta - \frac{py}{U} \right) 2ay dy \quad (3)$$

When Eqs. (1-3) are combined and integrated, we find that

$$M_{p\alpha} p\alpha = -16q C_{N\alpha} \alpha \delta \quad (4)$$

Here it may be noted that this "magnus effect" does not depend directly on roll rate, since p has canceled out. However, as will be seen below, the equilibrium roll rate is proportional to δ , so there is an indirect dependence on roll rate.

The magnus moment coefficient derivative $C_{M_{p\alpha}}$ plotted in Fig. 2 is defined by

$$M_{p\alpha} p\alpha = q\pi a^2 2a\alpha (pa/U) C_{M_{p\alpha}} \quad (5)$$

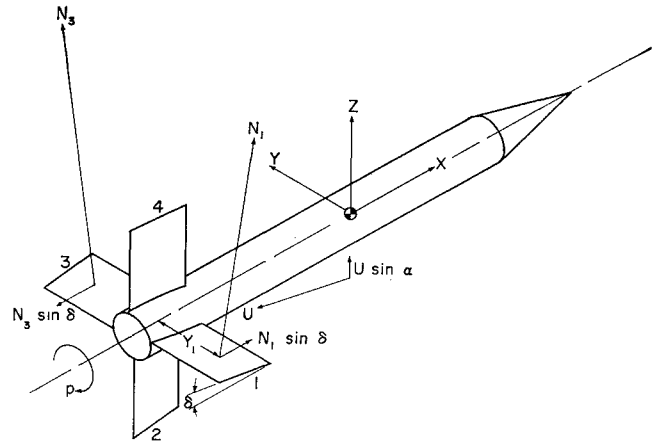


Fig. 3 Nomenclature and origin of present magnus moment

Consequently, from Eqs. (4) and (5),

$$C_{M_{p\alpha}} = -(8/\pi)(pa/\delta U)^{-1} C_{N\alpha} \quad (6)$$

The value of $pa/\delta U$ can be found by requiring that, since the missile is assumed to be in a steady-state rolling condition, the rolling moment on each panel due to the deflection δ is equal and opposite to the roll-damping moment, which is proportional to p :

$$\int_a^{3a} q C_{N\alpha} \left(\delta - \frac{py}{U} \right) 2ay dy = 0 \quad (7)$$

This equation gives

$$pa/\delta U = \frac{6}{13} = 0.462 \quad (8)$$

This value compares favorably with the experimental value of 0.497 that is implied by Fig. 16 of Ref. 1.

The value of $C_{N\alpha}$ appropriate to a rectangular wing is given by Harmon¹¹ as

$$C_{N\alpha} = 4[1 - (1/2AB)]/B \quad (9)$$

where A is the wing aspect ratio and $B = (M^2 - 1)^{1/2}$. Joining the two exposed fins together as one panel gives an aspect ratio of 2. Combination of Eqs. (6, 8, and 9) leads to

$$C_{M_{p\alpha}} = -5.52 C_{N\alpha} = -(22.1/B)[1 - (1/4B)] \quad (10)$$

Equation (10) has been plotted as the solid curve in Fig. 2. The agreement is reasonably good for the higher Mach numbers. Agreement should not be expected for Mach numbers lower than $M = (2)^{1/2} = 1.4$, for at this value the Mach line from the wing tip first intersects the wing-body juncture. Then the value of $C_{N\alpha}$ predicted by Eq. (9) is no longer correct, and wing-body interference must be important. However, this simple analysis does predict a magnus moment of the indicated sign, magnitude, and general trend with Mach number.

References

- ¹ Nicolaidis, J. D. and MacAllister, L. C., "A review of aeroballistic range research on winged and/or finned missiles," Ballistic TN 5, Bureau of Ordnance, Dept. of the Navy, Washington, D. C. (1955).
- ² Buford, W. E., "Magnus effect in the case of rotating cylinders and shell," Ballistic Research Lab., Memo Rept 821, Aberdeen Proving Ground, Md. (July 1954).
- ³ Martin, J. C., "On magnus effects caused by the boundary layer displacement thickness on bodies of revolution at small angles of attack," Ballistic Research Lab., Rept 870-Revised, Aberdeen Proving Ground, Md. (June 1955).
- ⁴ Platou, A. S., "The magnus force on a rotating cylinder in transonic cross flows," Ballistic Research Lab., Rept 1150, Aberdeen Proving Ground, Md. (September 1961).

⁵ Benton, E. R., "Wing tail interference as a cause of 'magnus' effects on a finned missile," *J Aerospace Sci* 29 1358-1367 (1962)

⁶ Platou, A. S., "The magnus force on a finned body," Ballistic Research Lab, Rept 1193, Aberdeen Proving Ground, Md (March 1963)

⁷ Nielsen, J. N., "Quasi-cylindrical theory of wing-body interference at supersonic speeds and comparison with experiment," NACA Rept 1252 (1955)

⁸ Nielsen, J. N., *Missile Aerodynamics* (McGraw-Hill Book Co Inc, New York, 1960), Chap 5

⁹ Ribner, H. S. and Malvestuto, F. S., "Stability derivatives of triangular wings at supersonic speeds," NACA TR 908 (1948)

¹⁰ Bolz, R. E., "Dynamic stability of a missile in rolling flight," *J Aeronaut Sci* 19, 395-403 (1952)

¹¹ Harmon, S. M., "Stability derivatives at supersonic speeds of thin rectangular wings with diagonals ahead of tip Mach lines," NACA Rept 925 (1949)

Length of the Laminar Hypersonic Wake during Ballistic Re-Entry

PAUL S. LYKODIS*

The Rand Corporation, Santa Monica, Calif

1 Introduction

MOST of the studies pertaining to the length of the wake of an object moving at hypersonic speeds in a dense atmosphere refer to steady-state conditions. The reason for this assumption is that one can prove that the decelerations involved are very small and contribute very little to the fluid mechanics of the problem. For instance, over a period of 10 sec an intercontinental ballistic missile of characteristic length, say of 10 ft, can cover a distance of the order of 100,000 ft. With these numbers one can easily see that in the equation of conservation of momentum the order of magnitude of the acceleration $\partial u/\partial t \sim (100,000 \text{ ft}/10 \text{ sec})/10 \sim 10^6 \text{ ft/sec}^2$ whereas the order of magnitude of the quantity $u(\partial u/\partial x) \sim (100,000 \text{ ft}/10 \text{ sec})^2/10 \text{ ft} \sim 10^7 \text{ ft/sec}^2$. For this reason one neglects the nonsteady term in the equation of motion (and similarly in the equations of conservation of mass and energy) and proceeds in solving the steady-state problem. As a matter of fact, since for certain calculations one is not interested in the details of the flow very close to the moving object, the assumption that the fluid moves inside the wake with a velocity of the order of 80% of the free-flight velocity is remarkably good.

The steady-state results may be interpreted in two ways. First, they may be understood in a system of coordinates fixed relative to the body; in this case we go downstream a distance x in order to measure (or calculate) such time independent quantities as electron concentration, wake width, and the like. Second, one may define a system of coordinates fixed at the laboratory, form a thin optical slit in front of him, and observe the temporal growth of the wake as the object passes by. It is obvious that if the velocity of the object is denoted by U , the coordinate x of the object-fixed system and the coordinate t of the laboratory system will be linked by the simple relation

$$x = Ut \quad (1)$$

Received October 4, 1963. Any views expressed in this paper are those of the author. They should not be interpreted as reflecting the views of The Rand Corporation or the official opinion or policy of any of its governmental or private research sponsors. Papers are reproduced by The Rand Corporation as a courtesy to members of its staff.

* Consultant; also Professor, School of Aeronautical and Engineering Sciences, Purdue University. Associate Fellow Member AIAA.

Now assume that the object does not move in a medium of constant mass density. Granted that the deceleration which the body will suffer does not influence its fluid mechanical aspects, the wake will develop temporally at each fixed altitude as if it had moved past that point with a constant velocity equal to the one it had when passing through this point. In order to find the length of the wake based on a given electron concentration n_e when the object is at point 2, we proceed as follows. Assume that the tail of the wake where the electron density becomes n is located at an altitude H_1 . From the ballistic diagram of the body (altitude vs velocity vs time for given ballistic coefficient and initial entry conditions) calculate U_1 and the time difference $t_2 - t_1$. Then calculate the length $U_1(t_2 - t_1)$. Knowing these numbers, use the steady-state theory to check if the electron density at the station x corresponding to the altitude H_1 and velocity U_1 is equal to n . If not, change the altitude H_1 to another one, and repeat this procedure until it is successful. The length based on this procedure we shall call the "ballistic wake length."

In the next paragraph we shall apply this method assuming thermodynamic equilibrium and a hemisphere-cylinder configuration. It goes without saying that this is a highly unrealistic model, but it can well serve as an example illustrating the error that can be made if one assumes that at a given altitude the wake's length is equal to the one that eventually would develop at that altitude if the body had stayed there moving with a constant speed. We shall call this last quantity the "constant altitude and velocity wake length."

The problem under discussion has been studied in Ref 1. The present work was undertaken in order to point out that what is called in Ref 1 the nonsteady solution is the steady one, properly understood, and also to show how results can be obtained in a closed form without the need of numerical integrations.

2 Calculation

We start with Eq (47) of Ref 2 which is duplicated below for ready reference:

$$\frac{h(x,0)}{RT_0} = \frac{h(0,0)/RT_0}{\left\{1 + \frac{[h(0,0)/RT_0]^{1/4} x}{0.53(\rho_\infty/\rho_0)U C_D r_0^2}\right\}^{0.8}} \quad (2)$$

$h(x,0)$ is the enthalpy at a station at distance x downstream located on the axis of symmetry. $h(0,0)$ is the value of the enthalpy at the station $x = 0$ where the gas has expanded to the ambient pressure and from there on can cool only through the mechanism of thermal conduction. R is the universal gas content, T_0 and ρ_0 are reference temperature and mass density. A discussion of the validity of the fore-mentioned equation can be found in Ref 2. We also recall from Ref 4, that within a good approximation, the following relation is valid:

$$\frac{h(0,0)}{RT_0} = \frac{(\gamma - 1)M^2}{6} \left(\frac{h_\infty}{RT_0} \right) \quad (3)$$

M is the Mach number of the freestream and γ may be taken equal to 1.4. Furthermore, let us assume that we deal with an isothermal atmosphere for which one can write

$$\rho_\infty/\rho_0 = e^{-\alpha H} \quad (4)$$

where α is an appropriate numerical constant ($\alpha = 4.15 \times 10^{-5} \text{ ft}^{-1}$) and H is the altitude. For the density distribution of Eq (4) and given initial conditions of altitude H_0 , velocity U_0 , and angle of entry θ one can trace diagrams of altitude vs velocity vs time as a function of the ballistic coefficient

$$\beta = W \sin \theta / C_D r_0^2 \quad (5)$$